UCLA

Title

Pre-synaptic C-terminal truncated tau is released from cortical synapses in Alzheimer's disease

Permalink

https://escholarship.org/uc/item/4r75w527

Authors

Sokolow, S
Henkins, KM
Bilousova, T
et al.

Publication Date

2015

DOI

10.1111/jnc.12991

Peer reviewed

ORIGINAL ARTICLE

Pre-synaptic C-terminal truncated tau is released from cortical synapses in Alzheimer's disease

Sophie Sokolow,*,†,‡,§ Kristen M. Henkins,* Tina Bilousova,* Bianca Gonzalez,* Harry V. Vinters,¶,** Carol A. Miller,†† Lindsey Cornwell,‡‡ Wayne W. Poon‡‡ and Karen H. Gylys*,†,‡,**

*UCLA School of Nursing, Los Angeles, California, USA

†UCLA Brain Research Institute, Los Angeles, California, USA

‡UCLA Center for the Advancement of Gerontological Nursing Sciences, Los Angeles, California, USA

§UCLA Clinical and Translational Science Institute, Los Angeles, California, USA

¶Departments of Pathology and Laboratory Medicine, David Geffen School of Medicine at UCLA, Los Angeles, California, USA

**Mary S. Easton Center for Alzheimer's Research at UCLA, Los Angeles, California, USA

††Departments of Pathology, Neurology, and Program in Neuroscience, Keck USC School of Medicine, Los Angeles, California, USA

‡‡Institute for Memory Impairments and Neurological Disorders, UC Irvine, Irvine, California, USA

Abstract

The microtubule-associated protein tau has primarily been associated with axonal location and function; however, recent work shows tau release from neurons and suggests an important role for tau in synaptic plasticity. In our study, we measured synaptic levels of total tau using synaptosomes prepared from cryopreserved human postmortem Alzheimer's disease (AD) and control samples. Flow cytometry data show that a majority of synaptic terminals are highly immunolabeled with the total tau antibody (HT7) in both AD and control samples. Immunoblots of synaptosomal fractions reveal increases in a 20 kDa tau fragment and in tau dimers in AD synapses, and terminal-specific antibodies show that in many synaptosome samples tau lacks a C-terminus. Flow cytometry experiments to quantify the extent of C-terminal truncation reveal that only 15–25% of synaptosomes are positive for intact C-terminal tau. Potassium-induced depolarization demonstrates release of tau and tau fragments from pre-synaptic terminals, with increased release from AD compared to control samples. This study indicates that tau is normally highly localized to synaptic terminals in cortex where it is well-positioned to affect synaptic plasticity. Tau cleavage may facilitate tau aggregation as well as tau secretion and propagation of tau pathology from the pre-synaptic compartment in AD.

Keywords: Alzheimer's disease, flow cytometry, synaptosome, tau cleavage, tau fragment, tau release.

J. Neurochem. (2015) **133**, 368–379.

In the tauopathy family of neurodegenerative diseases, which includes frontotemporal dementia, Pick's disease, and corticobasal degeneration, the microtubule-associated cytoskeletal protein tau forms intracellular aggregates. In Alzheimer's disease (AD), the most common tauopathy, hyper-phosphorylated tau (p-tau) aggregates into paired helical filaments, neuropil threads, and ultimately forms lesions known as neurofibrillary tangles (NFT). Tau is a highly soluble neuronal protein, primarily localized to axons, where it is well known to bind microtubules (MTs) through its C-terminal MT-binding domain and promote their stabilization (for review see Hanger *et al.* 2009; Gotz *et al.* 2013).

ORIGINAL ARTICLE

Given its hypothesized central role in regulation of axonal transport, it is interesting that tau deletion does not significantly alter longevity or phenotype in mice (Harada *et al.* 1994). Likewise, axonal transport is not impaired by tau knockout or tau over-expression *in vivo* (Yuan *et al.* 2008). Interestingly, the role of tau in relation to axonal transport associated with Aβ-mediated toxicity *in vitro* is still controversial. Indeed, studies have shown that tau is required for amyloid-beta (Aβ)-mediated reduction in axonal transport of mitochondria and the neurotrophin receptor TrkA in hippocampal neurons (Vossel *et al.* 2010). While others reported that tau is not required for the disruption of fast axonal transport of brain-derived neurotrophic factor in hippocampal neuronal culture (Ramser *et al.* 2013).

A number of studies suggest that tau plays a pathological role in dendritic spines. For example, when over-expressed in primary neuron cultures, tau missorts into the somato-dendritic compartment, resulting in loss of synaptic markers (Thies and Mandelkow 2007). Somatodendritic localization may also be driven by tau hyper-phosphorylation, which is thought to be a relatively early event that results in detachment from microtubules (Tashiro *et al.* 1997; Morris *et al.* 2011).

Other evidence suggests that tau mediates excitotoxicity through interactions with the tyrosine kinase fyn and its substrates PSD-95 and the *N*-methyl-D-aspartate (NMDA) receptor (Ittner *et al.* 2010). Such a role for tau in mediation of post-synaptic fyn localization may suggest a mechanism by which tau reduction protects against Aβ toxicity and excitotoxicity *in vivo* (Roberson *et al.* 2007).

More recently, Frandemiche *et al.*, (2014) reported that tau travels into the post-synaptic density in response to electrical stimulation in murine cortical cultures, and that Aβ blocks this tau recruitment into the synapse, suggesting tau involvement in synaptic plasticity. Also consistent with an important synaptic role for tau, Chen *et al.*, (2012) showed that tau protein regulates spine density upon brain-derived neurotrophic factor stimulation.

In addition to contributing to disease through a gain of toxic function by phosphorylation, some evidence suggests that tau toxicity may follow release from degenerating cells into the extracellular space (Gomez-Ramos *et al.* 2006; Frost *et al.* 2009). Fragments of tau cleaved at the C-terminal are present in the cerebrospinal fluid (CSF) collected from human AD subjects and from tau transgenic mice (Kim *et al.* 2010; Saman *et al.* 2012). In fact, Plouffe *et al.*, (2012) suggest that hyper-phosphorylation and C-terminal cleavage may favor tau secretion, propagation of tau pathology in the brain and ultimately tau buildup in the CSF. A more recent study indicates that N-truncated tau fragment (~ 20 kDa) is a CSF biomarker of neurodegenerative disease associated with memory impairment (Amadoro

et al. 2014b). Still, little is known about levels of cleaved tau in the pre-synaptic compartment.

We have previously demonstrated that p-tau co-localizes with Aβ in AD synapses and that p-tau species are mainly oligomeric (Fein *et al.* 2008; Henkins *et al.* 2012; Sokolow *et al.* 2012b). In the present study, we assessed total levels of tau protein and its cleaved fragments in surviving nerve terminals (i.e., with intact membranes) from cryopreserved human AD and control samples (Gylys *et al.* 2004b; Sokolow *et al.* 2012c). P-tau represents a small fraction of tau in synaptosomes, and tau is abundant in both cognitively normal and AD synapses, with a 20 kDa tau fragment and tau dimers elevated in AD samples. Most synaptic tau is cleaved at the C-terminus in both AD and control samples, with the level of C-terminal truncated tau higher in AD synaptosomes. Results also show increased depolarization-dependent tau release from AD synaptic terminals.

Materials and methods

Materials

Polystyrene microsphere size standards were purchased from Polysciences, Inc. (Warrington, PA, USA). Zenon mouse IgG Labeling kits for were purchased from Molecular Probes (Eugene, OR, USA). The monoclonal anti-Synaptosomal-Associated Protein 25 (SNAP-25) antibody was purchased from Sternberger Monoclonals, Inc. (Lutherville, MD, USA). Tau and p-tau antibodies used to immunolabeled our synaptosomal proteins (P-2) are listed in Table 1.

Human brain specimens

Parietal cortex (Brodmann area A39 and A40) samples with a postmortem interval (PMI) ≤ 15 h were obtained at autopsy from the Alzheimer's Disease Research Centers at University of California, Los Angeles, University of California, Irvine, and the University of Southern California. Each diagnosis was established clinically and histopathologically. The mean age for controls was 92.6, and for AD was 84.6; the age difference was significant ($p < 0.03$) and likely results from four cases over 90 years in the relatively small aged control group. Despite the age difference, all control cases were included in the present experiment because of the difficulty of obtaining short-PMI tissue (i.e., PMI ≤ 15 h) from clinically documented controls. The mean postmortem delay was 9.61 for controls and 7.29 for AD; these differences were not significant (Student's *t*-test). Samples were obtained and handled according to UCLA's Institutional Review Board and Environment, Health and Safety regulations.

Synaptosomes (P-2) preparation

Unfixed fresh samples (~ 0.3–5 g) were minced in 0.32 M sucrose the day of autopsy, slowly frozen and stored at −80°C until homogenization. The crude synaptosomal pellet (P-2) was prepared as described previously (Gylys *et al.* 2003; Sokolow *et al.* 2012a,c) briefly, the minced tissue was homogenized in 10 volume of 0.32 M

Table 1 List of tau and phosphorylated tau antibodies

Antibody	Type	Epitope	Source
HT7	Mouse monoclonal	aa 159–163	Pierce Biotechnology, Rockford, IL, USA
Tau 12 (N-terminal)	Mouse monoclonal	aa 9–18	Abcam, Cambridge, MA, USA
Tau 46 (C-terminal)	Mouse monoclonal	aa 428–441	Abcam, Cambridge, MA, USA
Phospho-PHF tau AT8	Mouse monoclonal	pSer202/pThr205	Pierce Biotechnology, Rockford, IL, USA
Phospho-PHF tau AT100	Mouse monoclonal	pSer212/pThr214	Pierce Biotechnology, Rockford, IL, USA
Phospho-PHF-1	Mouse monoclonal	pSer396/pSer404	Kindly provided by Dr. Peter Davies, Albert Eisntein College of Medicine, NY, USA
Phospho-S422 (pS422)	Rabbit polyclonal	pSer422	Biosource-Invitrogen-Life technologies, Carlsbad, CA, USA

sucrose containing protease and phosphatase inhibitors. The homogenate was first centrifuged at 1000 g for 10 min; the resulting supernatant was centrifuged at 10 000 g for 20 min to obtain the crude synaptosomal pellet (P-2).

Immunolabeling of P–2 pellet

P-2 aliquots were immunolabeled for flow cytometry analysis according to a method for staining of intracellular antigens (Schmid *et al.* 1991). Pellets were fixed in 0.25% buffered paraformaldehyde (1 h, 4°C) and permeabilized in 0.2% Tween 20/phosphate-buffered saline (PBS) (15 min, 37°C). Antibodies (Table 1) were labeled directly with Zenon kit Alexa Fluor 488 according to manufacturer instructions (Molecular Probes). Alexa 488 labeled antibody mixture was added to P-2 aliquots and incubated at 23°C for 30 min. Then, immunolabeled P-2 aliquots were washed 2 times with 1 mL 0.2% Tween20/PBS, spun (1310 g at 4°C), and resuspended in PBS buffer (0.75 mL) for flow cytometry analysis. The synaptosomal pellet was dispersed for all washes and for incubations with fixative, detergent, and antibody, then collected by centrifugation (1310 g at 4°C) as previously described (Gylys *et al.* 2000, 2004a; Fein *et al.* 2008; Sokolow *et al.* 2011, 2012a,b,c; Henkins *et al.* 2012). Negative controls are P-2 aliquots labeled with the appropriate isotype specific control antibody in order to accurately quantify specific immunolabeling. For the present experiments, all antibodies belong to IgG$_1$ subtype.

Flow cytometry

Data were acquired using an BD-FACS Calibur analytic flow cytometer (Becton-Dickinson, San Jose, CA, USA) equipped with argon 488 nm, helium-neon 635 nm, and helium-cadmium 325 nm lasers. At least 5000 events were collected and analyzed for each sample. Debris was excluded by establishing a size threshold set on forward light scatter as previously described (Gylys *et al.* 2004a; Sokolow *et al.* 2012c). Alexa 488 fluorochromes were detected by the LSR's FL1 photomultiplier tube detectors; instrument settings were identical for all samples in each experiment. Analysis was performed using FCS Express software (DeNovo Software, Ontario, Canada).

Synaptosome extracts and tau bead–based immunoassay

Washed P-2 fractions (~ 100 μg/sample) were first extracted by sonication in a detergent-free buffer (10 mM Tris, 1 mM EGTA, 10% sucrose, pH 7.5) and then spun at 25 000 g. The supernatant of this detergent-free extraction (Sup. A) was used to quantify the levels of aqueous soluble tau species. The remaining pellet was extracted by sonication in the same buffer containing 1% *N*-lauroylsarkosyl (NLS) and spun at 300 000 g. This supernatant was analyzed as the detergent-soluble fraction (Sup. NLS)(Sokolow *et al.* 2012a). The aqueous and detergent-soluble fractions were assayed for total tau using a bead-based immunoassay (INNO-BIA AlzBio3) purchased from Innogenetics (Ghent, Belgium). Assays were performed on a Luminex® instrument using X-map® Technology (Austin, TX, USA) and xPONENT software. Each extract was analyzed in duplicate as previously described (Ringman *et al.* 2008; Sokolow *et al.* 2012a).

Western blotting

P-2 aliquots were boiled in Laemmli loading buffer (2% sodium dodecyl sulfate [SDS], Invitrogen, Carlsbad, CA, USA) and electrophoresed on 4–20% Tris-glycine gradient gels. Membranes were blocked and immunolabeled as described previously (Sokolow *et al.* 2011, 2012a,c). Because common synaptic housekeeping proteins are altered in AD synapse, membranes were stained with either Coomassie blue or Ponceau to document equal protein loading; only membranes with equal loading were quantified. Immunolabeled proteins were visualized by enhanced chemiluminescence detection reagents. Resulting films were scanned and quantified on a UVP BioSpectrum 600 imaging system using VisionWorks Version 6.6A software (Upland, CA, USA).

Depolarization–induced tau release

Freshly made P2 samples (400 μg protein) were resuspended in 100 μL of Normal Kreb's solution (5.5 mM KCl, 160 mM NaCl, 1.2 mM MgCl$_2$, 1.5 mM CaCl$_2$, 10 mM HEPES, 10 mM Glucose 160 mM Na, pH 7.4) and pre-incubated for 30 min at 37°C. To depolarize, one half of the synaptosome contained solution was diluted 2-fold with depolarizing solution (100 mM KCl, 65 mM NaCl, 1.2 mM MgCl$_2$, 1.5 mM CaCl$_2$, 10 mM HEPES, 10 mM Glucose 160 mM Na, pH 7.4) for a final concentration of 50 mM. The other half was diluted with Normal Kreb's solution to a final concentration of 5 mM KCl (control). The samples were incubated for 30 min at 37°C and centrifuged at 2000 g for 4 min. Supernatants were collected, concentrated using Vivaspin 500 concentrators 10 kDa cut off (GE Healthcare, Little Chalfont, UK) and resolved by 10–20% Tris-Glycine gradient gel (Invitrogen) under reducing conditions followed by transferring to polyvinylidene difluoride membrane and probing with HT7 total tau antibodies.

Statistical analysis

Data are presented as means ± SEM. Student's *t*-tests were calculated using Microsoft Excel or the Vassarstat interactive statistical website (http://vassarstats.net/); Richard Lowry, Pough-keepsie, NY, USA). Tau release analyses were performed using analysis of variance and Bonferroni's *post hoc* multiple comparison tests (Sigma Plot 11.0, Systat Software, San Jose, CA, USA).

Results

Tau protein is abundant in normal and AD cortical synapses

Parietal cortex samples (Brodmann area 39 & 40; PMI < 12 h) were obtained from confirmed AD and control cases. Control cases included aged cognitively normal controls and neurologic controls with non-AD diagnoses (see Table 2). Synaptosomes are intact resealed nerve terminals, primarily pre-synaptic with some adherent post-synaptic structures, formed when fresh samples are gently homogenized in isotonic sucrose (Gylys *et al.* 2004a; Sokolow *et al.* 2012a,b, c). Synaptosome particles contain synaptic structures *in situ*, including mitochondria and exocytotic elements; the prepa-ration has been used for decades to study neurotransmitter release and synaptic function (Dunkley *et al.* 2008; Wilhelm *et al.* 2014).

The focus of the present study was to measure various forms of tau (i.e., non-phosphorylated, phosphorylated and cleaved) in AD compared to control synapses.

For the present experiments, samples were first cryopre-served and later homogenized to obtain the P-2 (crude synaptosome; synaptosome-enriched) fraction. Flow cytom-etry analysis was used to examine tau in a large and highly pure population (5000 events/sample) of human cortical synaptosomes within the P-2 fraction. Tau protein was quantified using the monoclonal antibody HT7, generated against normal and PHF-tau (total tau) from human and bovine brain; the epitope maps to residues 159–163 (Table 1), which is near the center of full-length tau. Figure 1a demonstrates a positive control sample immuno-labeled for the pre-synaptic docking protein SNAP-25. Background labeling is also illustrated for a representative sample in Fig. 1b. The positive control reveals the degree to which non-synaptic elements are excluded from analysis when a gate is drawn to include only particles between 0.75 and 1.5 microns on forward scatter, which is proportional to particle size. When collecting events based on size and the use of viability dyes (e.g., calcein-AM, fluo-4), we previ-ously documented the membrane integrity, the inclusion of mitochondria and exclusion of debris, and the ∼ 95% purity of synaptosomes in the P-2 (Gylys *et al.* 2000, 2004a; Sokolow *et al.* 2011, 2012a,c), which compares to ∼ 87% purity for gradient-purified synaptosomes (Wolf and Kapatos 1989).

Flow cytometry allows quantification of the size of the immunolabeled fraction (% positive) as well as the brightness of the immune-fluorescent signal [Relative Fluorescence Units (RFU)] for individual synaptosomes within each sample (Gylys *et al.* 2000; Sokolow *et al.* 2012b). High levels of tau labeling (∼ 75% positive terminals) are illustrated in representative aged normal control (Fig. 1c), and aged AD synaptosomes (Fig. 1d).The bar graph compares the mean levels of synaptic total tau and p-tau quantified by flow cytometry in AD versus control synap-tosomes (Fig. 1e). The positive fraction of HT7 immunola-beled tau protein was large, ∼ 75% positive, in both AD ($n = 7$) and control ($n = 5$) synapses (Fig. 1e). In contrast, p-tau immunoreactive species were relatively low (4–20% positive) but elevated in AD compared to normal synapses when labeled with either AT100 (19.73 ± 5.6 vs. 3.72 ± 1.2; $p \leq 0.03$) or pS^{422} (10.22 ± 2.0 vs. 3.32 ± 1.0; $p \leq 0.02$) antibodies (Fig. 1e).

To exclude the possibility that abundant synaptic tau is a feature unique to surviving terminals in aged and AD parietal cortex, we next examined total tau expression in AD synaptosomes isolated from parietal cortex, hippocam-pus, and cerebellum. We then compared total tau expression in these three brain regions (Fig. 1f). Similar to parietal cortex results, hippocampal and cerebellar synaptosomes display relatively high levels of tau, with no difference observed in the size of the positive fraction (left bars–% pos.); however, the brightness of labeling (right bars–RFU) was reduced by half in cerebellum compared to parietal cortex (58.52 ± 5.4 vs. 25.15 ± 3.3; RFU; $p \leq 0.001$; $N = 4$ and $N = 6$, respectively). No difference in RFU (47.69 ± 3.31; $N = 4$) versus (58.52 ± 6.90; $N = 7$) was observed between regions playing an important role in AD etiology (i.e., hippocampus and parietal cortex). Taken together, Fig. 1 e and f indicate that tau protein is abundant in both AD and normal cerebral samples; the elevated RFU for total tau in AD parietal cortex and hippocampus compared to the AD cerebellum likely reflects HT7 immunolabeling of hyperphosphorylated tau in regions affected by the disease.

Tau in synaptosomes is divided between soluble and detergent–soluble pools

Because tau is generally considered to be a soluble protein, we extended our flow cytometric observations, using a bead-based immunoassay to measure total tau level in aqueous (i.e., detergent-free) and detergent-soluble extracts. Sequen-tial extractions were performed on AD and normal P-2 fractions–the P-2 fraction (crude synaptosome or synapto-some-enriched fraction) was used to have sufficient tissue for analysis. For the preparation of the initial aqueous soluble extract, washed P-2 pellets were sonicated in detergent-free buffer (i.e., Tris/sucrose). The aqueous extract was then isolated by ultracentrifugation and the resulting pellet was then sonicated in buffer plus detergent (1% *N*-laurylsarcosyl) to produce the detergent-soluble lysate (NLS).

Table 2 Case information for immunoblotting analysis

Lane		Sex	Age	PMI (h)	Braak & Braak score	Parietal tau pathology
	Normal cases					Sparse NFT (Gallyas)
1	726	F	97	5.5	–	0 NFT (Gallyas)
2	774	M	93	6	–	0 NFT (Gallyas)
3	779	F	88	12	–	0 NFT (Gallyas)
	15–09[a]	M	82	14.9	N with hippocampal sclerosis	0 (PHF1 ICC)
	726	F	97	8.5	–	0 NFT (Gallyas)
4	789[ab]	F	105	9	–	0 NFT (Gallyas)
	758[ab]	M	93	8.5	–	0 NFT (Gallyas)
	824[b]	F	86	12.5	–	0 NFT (Gallyas)
	PD Cases					
5	711	M	74	7.8	PD	0 NFT (Gallyas)
6	720	M	63	3.5	PD vs. Lewy body AD 2 year dementia	Sparse neurpil threads (Gallyas)
7	024 tauopathy	F	72	5	Dementia	
	AD cases					
8	782	F	89	12	IV–V; 10 year dementia	Freq NFT; sparse neuropil threads (Gallyas)
9	028[a]	F	91	7	VI; 7 year dementia	Abundant NFT; dense neuropil threads (tau ICC)
10	102	F	80	11	VI; 7 year dementia	Mod-high NFT; prom. neuropil threads (tau ICC)
11	716[a]	F	86	5	VI; 11 year dementia	Freq NFT; sparse neuropil threads (Gallyas)
12	730	F	76	3.6	VI; 26 year dementia	Freq NFT; freq neuropil threads (Gallyas)
13	718[a]	M	83	7	V; 2 year dementia	Mod NFT; mod neuropil threads (Gallyas)
14	776	F	99	11.5	V; 2 year dementia	Sparse NFT (Gallyas)
	809[a]	M	65	5.5	V; 11 year dementia	Freq NFT; mod neuropil threads (Gallyas)
	731[a]	F	87	10	V; 5 year dementia	Mod NFT; sparse neuropil threads (Gallyas)
	10–09[a]	F	82	4.5	V	+++ NFT (PHF-1 ICC)
	9–09[a]	M	87	6	V	0 NFT (PHF-1 ICC)
	8–12[b]	M	92	4	II	0 NFT (PHF-1 ICC)
	22–12[b]	M	93	6.5	–	0 NFT (PHF-1 ICC)
	37–11[b]	F	94	8	VI	++ NFT (PHF-1 ICC)
	12–12[b]	F	82	7	VI	++ NFT (PHF-1 ICC)

Lane column refers to Fig. 2b; [a]Fig. 3; [b]Fig. 4.

Using this technique, we have previously reported p-tau to be elevated in the aqueous and NLS extracts derived from AD synapses compared to controls (Henkins *et al.* 2012). In this present analysis, total tau did not differ between aged normal controls and AD samples in either extracts (Fig. 2a). Total tau was evenly distributed between the two fractions, with ~ 45% of the total tau level in the aqueous and 55% in the detergent-soluble fractions for both AD and normal cases (data not shown). These results indicate that in aged normal control and AD synapses, a significant fraction of synaptic tau requires detergent solubilization.

Tau dimers and a 20 kDa fragment are elevated in AD synapses

To further extend our flow cytometric observations, we next examined the molecular weight of all tau forms present in nerve terminals using immunoblotting technique. We have previously documented a ~ two-fold enrichment for pre- and post-synaptic proteins in washed P-2 fractions (Sokolow

et al. 2012a), and we have also demonstrated the high degree of correlation between flow cytometry ('pure' synaptosomes') and Western blot measures of Aβ and p-tau peptides (Fein *et al.* 2008; Sokolow *et al.* 2012a,c).

In the present study, our immunoblots included P-2 fractions from a series of AD ($N = 7$) and aged normal control ($N = 4$) parietal cortex samples (Fig. 2b; case information and lane number for Fig. 2 is indicated in Table 2). The series also included three non-AD comparison cases, two with Parkinson's disease (PD), and a tauopathy case without diffuse or neuritic plaques that showed striking tau-immunoreactive neurofibrillary tangles and neuropil threads on neuropathological examination (Table 2). The neurologic controls (i.e., aged normal control, PD, and tauopathy) were included to determine the disease specificity of synaptic pathology in AD, and to document mixed pathology. For example, one of the PD cases displayed mixed pathology with a 2-year history of dementia; a Lewy body AD diagnosis was considered for this case. Of a note, we have previously reported a detailed
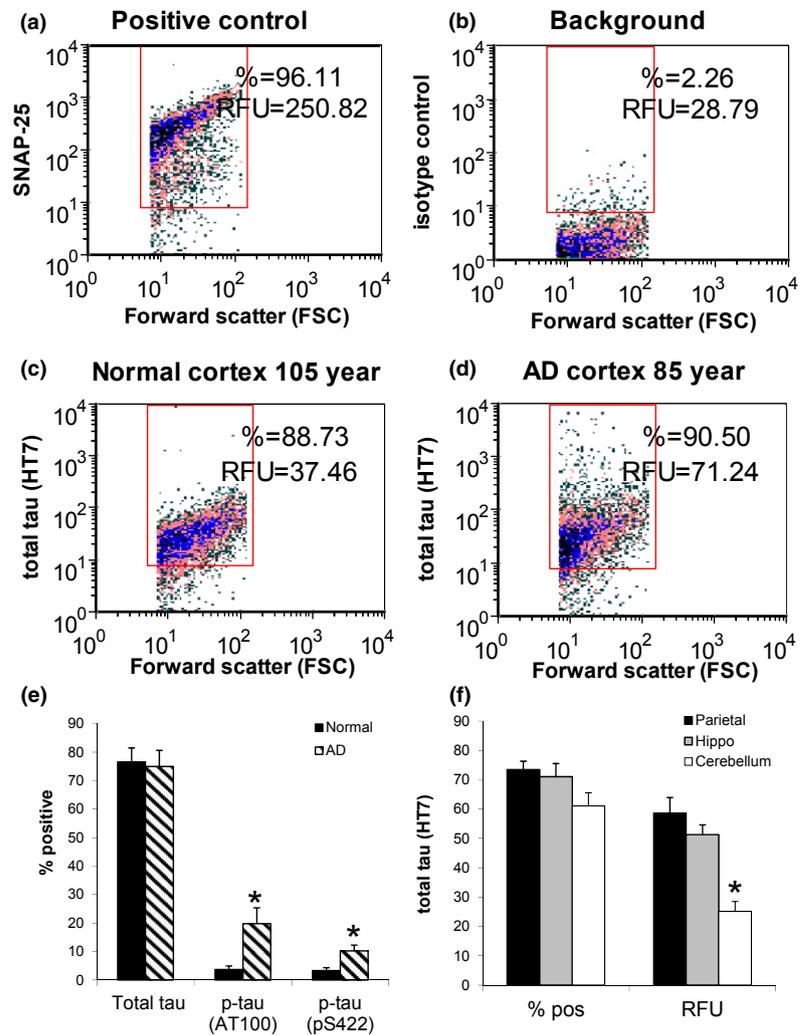
(a) Positive control — SNAP-25 vs Forward scatter (FSC); %=96.11, RFU=250.82

(b) Background — isotype control vs Forward scatter (FSC); %=2.26, RFU=28.79

(c) Normal cortex 105 year — total tau (HT7) vs Forward scatter (FSC); %=88.73, RFU=37.46

(d) AD cortex 85 year — total tau (HT7) vs Forward scatter (FSC); %=90.50, RFU=71.24

(e) % positive — Normal, AD; Total tau, p-tau (AT100)*, p-tau (pS422)*

(f) total tau (HT7) — Parietal, Hippo, Cerebellum; % pos, RFU*

Fig. 1 *Flow cytometry analysis of tau and p-tau in AD and aged control synaptosomes:* Representative density plots in an AD parietal cortex sample immunolabeled for SNAP-25 as a positive control and indicator of synaptosomal purity (a) and non-immune IgG (b), and representative density plots compare tau immunolabeling with the HT7 antibody in an aged normal control case (c), and an AD case (d). (e) Size of positive synaptosome fraction for the total tau (HT7) and p-tau antibodies (AT100, pS^{422}) in aged controls ($n = 5$) and AD cases ($n = 7$); (f) Size of positive synaptosome fraction (left bars) and brightness of immunolabeled synpatosomes with total tau (HT7) (RFU, relative fluorescence units–right bars) for the AD parietal cortex ($N = 4$), hippocampus ($N = 7$) and cerebellum ($N = 6$) samples; data were collected from 5000 terminals for each sample, *$p < 0.05$.

examination of Aβ peptide species in the same set of cases (Sokolow *et al.* 2012a).

Our analysis of synaptosomal tau immunodetection with HT7 antibody revealed that the major immunoreactive band was the extended tau form (~ 55 kDa; Fig. 2b). No difference in total tau expression was observed in AD versus controls (Fig. 2c). A ladder of probably tau fragment bands ranging from 35–50 kDa were also observed in controls and to a lesser extend in AD (Fig. 2b). Consistent with recent observations in AD homogenates (Patterson *et al.* 2011), an immunoreactive band at ~ 120 kDa was observed in most AD cases (relative intensity 50.54 vs. 1.19; $p \leq 0.001$) and indicates the presence of tau dimers in AD synapses (Fig. 2b and c). Another major immunoreactive band was consistently observed at about 20 kDa, and this tau truncated fragment was increased in AD compared to aged control samples ($p < 0.01$; ± 16.7 vs. 35.28 ± 4.2; $p \leq 0.04$; Fig. 2b and c). Alpha-synuclein (α-syn), a pre-synaptic protein localized to synaptic vesicles, was reduced in AD synaptosomal fractions

($p < 0.05$), and likely reflects synapse loss and dysfunction in surviving synapses (Fig. 2b and c).

Most synaptic tau is truncated at the C-terminus

Because evidence indicates that cleavage of tau, particularly by caspases, plays an important role in tau aggregation (Gamblin *et al.* 2003; Rissman *et al.* 2004; Ding *et al.* 2006; Yin and Kuret 2006; Wang *et al.* 2007; de Calignon *et al.* 2010; Zhang *et al.* 2014) and secretion (Plouffe *et al.* 2012), we next immunolabeled synaptosomes with specific antibodies directed either at the tau N- or C-terminus (tau 12 and tau 46, respectively; Fig. 3).

We first quantified the levels of N-term and C-term tau using flow cytometry analysis. Representative aged normal and AD samples immunolabeled with the N-terminal antibody (tau 12) are illustrated in Fig. 3a and b respectively, and the analysis with the C-terminal antibody (tau 46) is shown in Fig. 3c and d. The aggregate data confirm the abundance of synaptic tau with ~ 65–80% of synaptosomes immunopositive for the tau
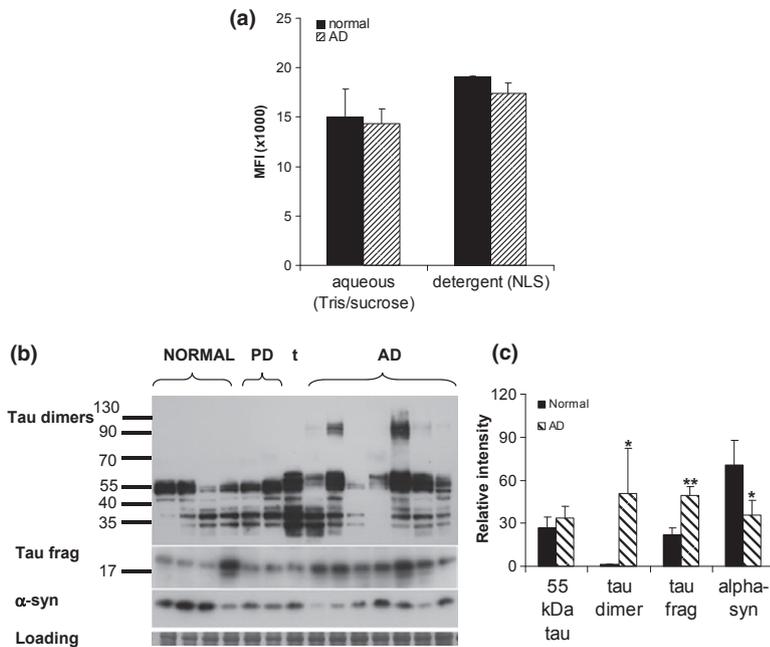
Fig. 2 *Biochemical analysis of tau in synaptosome-enriched fractions (SEF, P-2, crude synaptosomes):* (a) Distribution of tau in sequential buffer and detergent (1% *N*-laurylsarcosyl) extracts measure by bead-based immunoassay: MFI = mean fluorescent intensity (b) Western blot analysis of tau peptides (HT7 antibody) in a series of aged normal control ($N = 4$) and AD samples ($N = 7$). Controls include 2 Parkinson's disease cases and 1 tauopathy case (t); the right PD case (lane 6) had a 2-year history of dementia; case information is presented in Table 2 (c) Quantification of Western blot in B; *$p < 0.05$, **$p < 0.01$.

12 N-terminus antibody (Fig. 3e– left bars). In contrast, only 15–25% of synaptosomes in AD and control synapses were immunoreactive for the tau 46 C-terminus antibody (Fig. 3f– right bars). A significant increase in C-terminal tau immunofluorescence in AD compared to aged normal synapses is revealed in Fig. 3f (right bars). A trend for an increase in the N-terminal tau immunofluorescence in AD ($p > 0.05$) is also reported in Fig. 3f (left bars). Observed C- and N-terminal tau levels did not correlate with the case PMI (data not shown). Experiments with an antibody directed against tau cleaved at aspartate 421 (D421) did not reveal a difference in caspase-cleaved tau in AD (data not shown), suggesting synaptic C-terminal tau cleavage is not associated with altered caspase activity.

Using the tau 12 and tau 46 antibodies, P-2 preparations were next analyzed by Western blot to obtain size information (Fig. 3g and h). On immunoblots probed with tau 12, tau species with an intact N-terminus occurred in a group of bands ranging from 40 to 53 kDa. In addition, SDS-stable tau oligomers with a smeared appearance were detected with tau 12 in two aged control cases (lanes 1 & 2) and three AD cases (lanes 9, 12 &14; Fig. 3g). Longer exposures with this antibody revealed oligomerization in all AD and PD cases including the tauopathy case (data not shown).

Confirming flow cytometry analysis, when synaptosomal preparations were probed with tau 46, low levels of full-length tau with an C-terminal domain (40–55 kDa) were detected in both control and AD cases. Additionally, there were no tau 46 immunoreactive tau fragments (Fig. 3h).

Taken together, our immunoblotting results suggest that cleaved tau oligomers and tau dimers, detected with total tau antibody HT7, are mainly truncated at the tau C-terminus and preferentially accumulate in AD synapses (Fig. 2b).

Depolarization–induced release of pre–synaptic tau

To determine whether tau is released from the pre-synaptic compartment following KCl-induced depolarization, we used cryopreserved P-2 aliquots from postmortem AD and normal cases (Table 2). Immunoblots blots with the HT7 antibody were used to assess synaptosomal tau release into the supernatant following depolarization with Kreb's buffer containing 50 mM KCl. As illustrated in Fig. 4a, the extended tau form (~ 55 kDa), the truncated tau fragment (~ 20 kDa) as well as other N-terminal tau fragments (35–50 kDa) are released following depolarization. We quantified full-length tau by measuring the relative intensity of HT7 immunodetection signal. Two-way ANOVA revealed a significant treatment × diagnosis interaction [$F(1, 12) = 4.94$, $p < 0.046$]. Higher levels of tau are released from AD nerve terminals stimulated with KCl 50 mM (4092.3 ± 950.1, $N = 5$) compared to control cases (682.7 ± 255.8, $N = 3$, $p = 0.001$) (Fig. 4b). Tau release was also significantly higher in AD synaptosomes stimulated with KCl 50 mM (depolarizing Kreb's buffer; dep) (4092.3 ± 950.1) compared to baseline release (normal Kreb's–5 mM KCl; con) (1252.2 ± 197.2, $N = 5$, $p = 0.002$). There was no difference in tau release between both conditions in control synaptosomes (414.3 ± 65.3 vs.682.7 ± 255.8, at 5 and 50 mM KCl respectively, $N = 3$, $p > 0.05$).Our findings
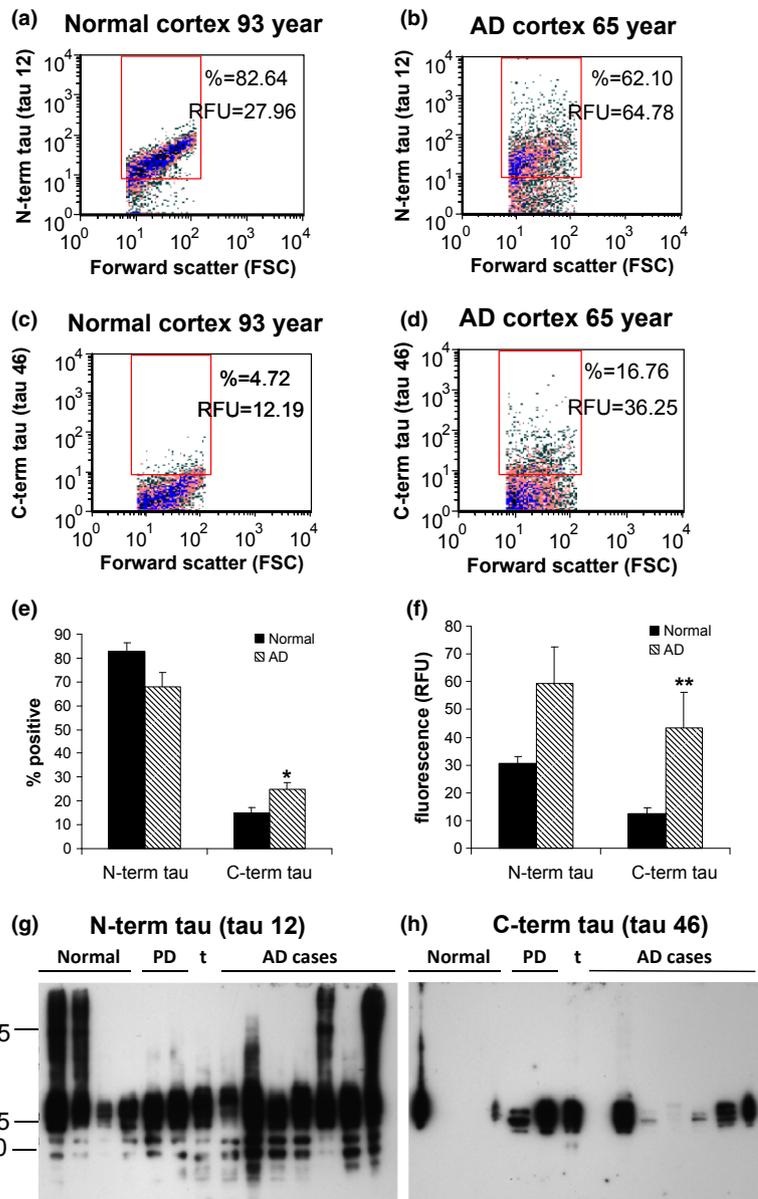
Fig. 3 *C-terminal truncation of synaptic tau:* (a–f) Flow cytometry analysis for a series of aged normal controls (*N* = 3) and AD (*N* = 6) cases; data were collected from 5000 terminals for each sample. Representative density plots are shown for a normal control (a) and an AD (b) sample immunolabeled with an antibody against the tau N-terminus (tau 12), and for a normal (c) and an AD (d) sample labeled for the tau C-terminus (tau 46). (e) Percentage of synaptosomes detected with an intact N- and C-terminus; (f) Brightness of fluorescence for N- and C-terminal tau (RFU, relative fluorescence units); *p* < 0.05, **p* < 0.01. (g and h) Western analysis of SDS-PAGE is shown for tau with an intact N-terminus (tau 12; g) and intact C-terminus (tau 46; h) for a series of aged normal control (*N* = 4) and AD samples (*N* = 7). Controls include 2 Parkinson's disease cases and 1 tauopathy case (t); case information (same as for Fig. 2b) is presented in Table 2.

indicate that AD synaptosomes are more susceptible to KCl-induced depolarization compared to control synaptosomes (Fig 4a and b).

Discussion

Tau protein is a critical player in AD pathogenesis (Rapoport *et al.* 2002; Roberson *et al.* 2007), but little is known about tau and other structural proteins in the synaptic compartment. In the current study using human synaptosomes isolated from aged control and AD cerebra, we made three important discoveries about synaptic tau. First, we demonstrate that tau is abundant in the synaptic compartment. Our flow cytometry experiments using total tau antibody showed that tau is present at high levels in

~ 75% of both normal and AD synapses. This finding suggests that high level of synaptic tau is not associated directly with AD pathology, as similar tau levels are observed in aged control and cerebellar synapses. Second, we showed that the main synaptic tau species found in normal and AD are C-truncated. Significantly higher percentage of AD terminals were positive for C-terminal-truncated tau compared to controls. In addition, higher levels of tau fragments and dimers were present in AD synaptosomes and are likely to contribute to tau aggregation and downstream pathology. Third, we demonstrated that tau peptides are released from control and AD synaptic terminals following depolarization. Interestingly, we found that higher levels of tau are released from AD nerve terminals compared to controls. The latest has
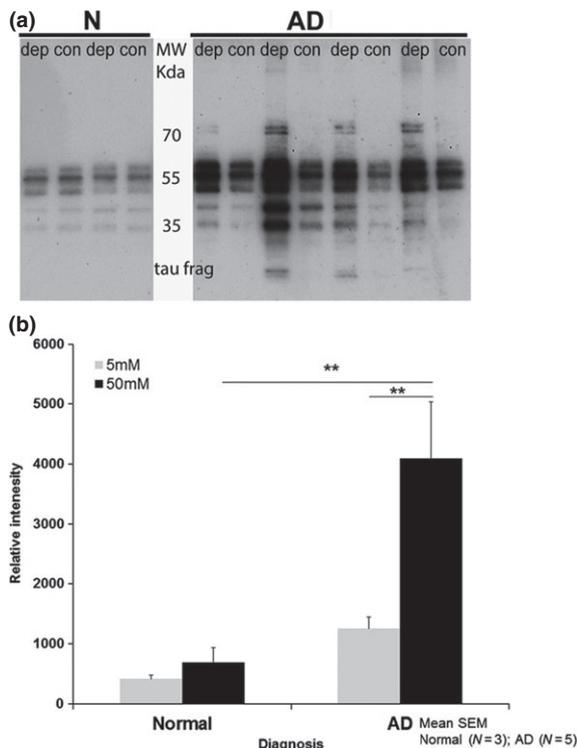
Fig. 4 *Depolarization-induced tau release from AD and control nerve terminals*: (a) P-2 samples were incubated 5 min with 50 mM KCl depolarizing solution (dep) or 5 mM KCl control buffer (con). Western SDS-PAGE analysis of supernatants using the HT7 antibody is shown. N are cognitively normal cases, AD are late-stage AD cases. (b) Bar graph illustrating tau release following KCl-induced depolarization. Each bar represents the mean ($\pm$ SEM), **$p < 0.01$.

important implications for current hypotheses about the spread of tau pathology in AD.

Tau is most often considered in the context of microtubule stabilization and is well known to be localized to axons in normal neurons (for review see; Morris *et al.* 2011). But the translocation of tau in the synaptic compartment was recently reported by Frandemiche *et al.,* (2014) who also suggested different tau dynamics between synapses containing or lacking Aβ. In the current study, biochemical measures of total tau confirm the abundance of tau species (e.g., full length, dimers, and fragments) in synapses. The abundance of synaptic tau could follow from release from interior endosomal/lysosomal compartments, a widespread system within synapses and activated in AD brain (Cataldo *et al.* 1995; Bernstein *et al.* 1996; Nixon *et al.* 2000, 2005). Additionally, we showed that detergent solubilization is required to measure approximately half the tau in synapses. Tau is a primary component of insoluble deposits in AD and other tauopathies, but is generally considered to

be a highly soluble protein that is resistant to aggregation in the absence of disease. Because tau is detergent-soluble in both aged normal control and AD synapses, our results indicate membrane interaction and/or localization within intraterminal endosomes that may influence tau function within the synapse. Reduced solubility or altered localization may also be age-related, and may provide an explanation for some of the age dependence of multiple tauopathies. Alternatively, detergent-extracted synaptic tau may reflect plasma membrane and lipid raft-associated tau that may contribute to signal transduction (Leugers and Lee 2010).

We and others have previously reported the presence of synaptic tau oligomers, which have been suggested as toxic intermediates that occur prior to intraneuronal fibril and tangle formation (Maeda *et al.* 2006, 2007; Sahara *et al.* 2007; Lasagna-Reeves *et al.* 2010; Meraz-Rios *et al.* 2010; Henkins *et al.* 2012; Tai *et al.* 2012) and mediate synaptic and mitochondrial dysfunction (Lasagna-Reeves *et al.* 2011). Tau oligomers have been identified *in vivo* and *in vitro*; on immunoblots with p-tau antibodies SDS-stable tau oligomers generally appear as dimers or trimers; native *in vitro* oligomers have been observed to be ~ 1843 kDa, corresponding to 40 molecules of tau (Maeda *et al.* 2007). In AD brains, a smeared appearance is sometimes observed for SDS-stable tau oligomers, indicating the presence of modified and fragmented forms of tau along with full-length tau in AD (Maeda *et al.* 2006; Henkins *et al.* 2012). The importance of soluble tau oligomers is highlighted by the recent observation that curcumin treatment suppresses soluble tau dimers in aged human tau transgenic mice (Ma *et al.* 2013).

There is controversy in the literature with respect to tau fragments, with a number of reports suggesting that a calpain-cleaved 17 kDa fragment is neurotoxic *in vivo* (Roberson *et al.* 2007) and in primary neuronal cultures (Park and Ferreira 2005). However, characterization by Garg *et al.,* (2011), suggests that the '17 kDa' fragment is really smaller (10.7 kDa), and is induced by other stressors (e.g., glutamate, thapsigargin) than Aβ; these authors conclude that this fragment is not toxic to cultured neurons. Cleavage of tau by caspase has also been suggested as an early event in tangle formation (Rissman *et al.* 2004); in particular, a caspase-truncated (Asp 421) tau fragment that has been observed in NFTs and dystrophic neurites in AD brain (Gamblin *et al.* 2003). More recently, the same caspase cleavage event was observed to occur just before tangle formation *in vivo*, and subsequently led to intracellular aggregates, phosphorylation, and recruitment of full-length tau into the aggregate (de Calignon *et al.* 2010). In Hela cells over-expressing human tau, caspase cleavage at the C-terminus occurs prior to tau secretion (Plouffe *et al.* 2012). However, we did not detect caspase-cleaved tau in our experiments, suggesting that other proteases may contribute more to tau aggregations in the synapse. Alternatively,

additional cleavage events may alter the D421 epitope over time in our primarily late-stage AD samples, or subsequent tau aggregations may obscure its detection.

The fragment we observe seems closer to 20 kDa, and a good deal of evidence links a 20–22 kDa NH2- tau fragment to synaptic dysfunction via disruption of mitophagy and mitochondrial dynamics (Amadoro *et al.* 2010, 2012, 2014a). This tau fragment was recently reported as a potential biomarker of neurodegenerative diseases associated with cognitive decline(Amadoro *et al.* 2014b), and seems most likely to correspond with the fragment we observe in AD synaptic terminals. Because C-terminal truncation occurs in control as well as AD synapses, the PMI may also contribute to tau fragmentation in human studies. However, the large literature associating tau fragments with downstream toxicity signaling and the lack of correlation of either fragment with the PMI argues against this explanation.

Our finding that depolarization-induced release of tau from AD nerve terminals provides direct evidence that tau is released from the synaptic compartment and is consistent with a large body of evidence that extracellular tau may be toxic (Gomez-Ramos *et al.* 2006; Karch *et al.* 2012). We have previously confirmed a long history of electron microscopy (EM) evidence documenting spherical pre-synaptic nature of synaptosomes (Dunkley *et al.* 2008; Fein *et al.* 2008; Wilhelm *et al.* 2014); pre-synaptic release is consistent with recent results that extracellular tau levels are regulated by neuronal activity (Yamada *et al.* 2014). In particular, increased tau release by AD synapses documents a mechanism long observed in human pathology and shown *in vivo* for the regional spread of tau pathology (Braak and Del Tredici 2011; de Calignon *et al.* 2012; Liu *et al.* 2012). Interestingly, neuron-to-neuron propagation of distinct strains of misfolded tau has recently been shown (Frost *et al.* 2009; Sanders *et al.* 2014). Release of tau from neurons and/or synapses is also in line with the finding that total tau and p-tau are increased in CSF of patients with AD, particularly those with rapidly progressing dementia (Johnson *et al.* 1997; van Rossum *et al.* 2012). Since CSF levels of tau and p-tau are widely considered to be among the most useful biomarkers for neurodegeneration, it seems likely that high synaptic levels of tau contribute to elevations in extracellular and CSF tau during synapse loss and cell death. Indeed, tau has recently been shown to be elevated in brain extracellular fluid and predict adverse outcome after traumatic brain injury in a small group of intensive care unit patients (Magnoni *et al.* 2012). Extracellular tau has also been associated with exosomes (Saman *et al.* 2012, 2014), underscoring the importance of understanding the relative contributions of passive tau release and tau that is released as a consequence of neuronal or synaptic loss.

Tau ablation does not produce major neurologic deficits (Morris *et al.* 2011), and a number of studies have shown that tau is required for the full expression of AD pathology in animal models (Santacruz *et al.* 2005; Roberson *et al.* 2007,

2011; Andrews-Zwilling *et al.* 2010; Ittner *et al.* 2010). Our data indicate that in AD, C-terminal truncation and fragmentation of synaptic tau are likely to further exacerbate tau aggregation and synaptic dysfunction. The present results reveal that tau is abundant in the pre-synaptic compartment and can also be released from the synapse. This previously unrecognized pool of cleaved and released tau would be expected to significantly impact synapse dysfunction and loss in AD as well as the propagation of tau pathology within the brain. Continued study of tau release mechanisms operating in the synaptic compartment is vital for identification of novel therapeutic targets.

Acknowledgments and conflict of interest disclosure

References

Amadoro G., Corsetti V., Stringaro A. *et al.* (2010) A NH2 tau fragment targets neuronal mitochondria at AD synapses: possible implications for neurodegeneration. *J. Alzheimers Dis.* 21, 445–470.

Amadoro G., Corsetti V., Atlante A., Florenzano F., Capsoni S., Bussani R., Mercanti D. and Calissano P. (2012) Interaction between NH(2)-tau fragment and Abeta in Alzheimer's disease mitochondria contributes to the synaptic deterioration. *Neurobiol. Aging*, 33, 833 e831–825.

Amadoro G., Corsetti V., Florenzano F. *et al.* (2014a) AD-linked, toxic NH2 human tau affects the quality control of mitochondria in neurons. *Neurobiol. Dis.*, 62, 489–507.

Amadoro G., Corsetti V., Sancesario G. M., Lubrano A., Melchiorri G., Bernardini S., Calissano P. and Sancesario G. (2014b) Cerebrospinal fluid levels of a 20–22 kDa NH2 fragment of human tau provide a novel neuronal injury biomarker in Alzheimer's disease and other dementias. *J. Alzheimers Dis.* 42, 211–226.

Andrews-Zwilling Y., Bien-Ly N., Xu Q. *et al.* (2010) Apolipoprotein E4 causes age- and Tau-dependent impairment of GABAergic interneurons, leading to learning and memory deficits in mice. *J. Neurosci.* 30, 13707–13717.

Bernstein H. G., Kirschke H., Wiederanders B., Pollak K. H., Zipress A. and Rinne A. (1996) The possible place of cathepsins and cystatins in the puzzle of Alzheimer disease: a review. *Mol. Chem. Neuropathol.* 27, 225–247.

Braak H. and Del Tredici K. (2011) Alzheimer's pathogenesis: is there neuron-to-neuron propagation? *Acta Neuropathol.* 121, 589–595.

de Calignon A., Fox L. M., Pitstick R., Carlson G. A., Bacskai B. J., Spires-Jones T. L. and Hyman B. T. (2010) Caspase activation precedes and leads to tangles. *Nature*, **464**, 1201–1204.

de Calignon A., Polydoro M., Suarez-Calvet M. *et al.* (2012) Propagation of tau pathology in a model of early Alzheimer's disease. *Neuron*, **73**, 685–697.

Cataldo A. M., Barnett J. L., Berman S. A., Li J., Quarless S., Bursztajn S., Lippa C. and Nixon R. A. (1995) Gene expression and cellular content of cathepsin D in Alzheimer's disease brain: evidence for early up-regulation of the endosomal-lysosomal system. *Neuron*, **14**, 671–680.

Chen Q., Zhou Z., Zhang L. *et al.* (2012) Tau protein is involved in morphological plasticity in hippocampal neurons in response to BDNF. *Neurochem. Int.* **60**, 233–242.

Ding H., Matthews T. A. and Johnson G. V. (2006) Site-specific phosphorylation and caspase cleavage differentially impact tau-microtubule interactions and tau aggregation. *J. Biol. Chem.* **281**, 19107–19114.

Dunkley P. R., Jarvie P. E. and Robinson P. J. (2008) A rapid Percoll gradient procedure for preparation of synaptosomes. *Nat. Protoc.* **3**, 1718–1728.

Fein J. A., Sokolow S., Miller C. A., Vinters H. V., Yang F., Cole G. M. and Gylys K. H. (2008) Co-localization of amyloid beta and tau pathology in Alzheimer's disease synaptosomes. *Am. J. Pathol.* **172**, 1683–1692.

Frandemiche M. L., De Seranno S., Rush T., Borel E., Elie A., Arnal I., Lante F. and Buisson A. (2014) Activity-dependent tau protein translocation to excitatory synapse is disrupted by exposure to amyloid-Beta oligomers. *J. Neurosci.* **34**, 6084–6097.

Frost B., Jacks R. L. and Diamond M. I. (2009) Propagation of tau misfolding from the outside to the inside of a cell. *J. Biol. Chem.* **284**, 12845–12852.

Gamblin T. C., Chen F., Zambrano A. *et al.* (2003) Caspase cleavage of tau: linking amyloid and neurofibrillary tangles in Alzheimer's disease. *Proc. Natl Acad. Sci. USA*, **100**, 10032–10037.

Garg S., Timm T., Mandelkow E. M., Mandelkow E. and Wang Y. (2011) Cleavage of Tau by calpain in Alzheimer's disease: the quest for the toxic 17 kD fragment. *Neurobiol. Aging*, **32**, 1–14.

Gomez-Ramos A., Diaz-Hernandez M., Cuadros R., Hernandez F. and Avila J. (2006) Extracellular tau is toxic to neuronal cells. *FEBS Lett.* **580**, 4842–4850.

Gotz J., Xia D., Leinenga G., Chew Y. L. and Nicholas H. (2013) What Renders TAU Toxic. *Front. Neurol.* **4**, 72.

Gylys K. H., Fein J. A. and Cole G. M. (2000) Quantitative characterization of crude synaptosomal fraction (P-2) components by flow cytometry. *J. Neurosci. Res.* **61**, 186–192.

Gylys K. H., Fein J. A., Tan A. M. and Cole G. M. (2003) Apolipoprotein E enhances uptake of soluble but not aggregated amyloid-beta protein into synaptic terminals. *J. Neurochem.* **84**, 1442–1451.

Gylys K. H., Fein J. A., Yang F. and Cole G. M. (2004a) Enrichment of presynaptic and postsynaptic markers by size-based gating analysis of synaptosome preparations from rat and human cortex. *Cytometry A*, **60**, 90–96.

Gylys K. H., Fein J. A., Yang F., Wiley D. J., Miller C. A. and Cole G. M. (2004b) Synaptic changes in Alzheimer's disease: increased amyloid-beta and gliosis in surviving terminals is accompanied by decreased PSD-95 fluorescence. *Am. J. Pathol.* **165**, 1809–1817.

Hanger D. P., Seereeram A. and Noble W. (2009) Mediators of tau phosphorylation in the pathogenesis of Alzheimer's disease. *Expert Rev. Neurother.* **9**, 1647–1666.

Harada A., Oguchi K., Okabe S. *et al.* (1994) Altered microtubule organization in small-calibre axons of mice lacking tau protein. *Nature*, **369**, 488–491.

Henkins K. M., Sokolow S., Miller C. A., Vinters H. V., Poon W. W., Cornwell L. B., Saing T. and Gylys K. H. (2012) Extensive p-tau pathology and SDS-stable p-tau oligomers in Alzheimer's cortical synapses. *Brain Pathol.* **22**, 826–833.

Ittner L. M., Ke Y. D., Delerue F. *et al.* (2010) Dendritic function of tau mediates amyloid-beta toxicity in Alzheimer's disease mouse models. *Cell*, **142**, 387–397.

Johnson G. V., Seubert P., Cox T. M., Motter R., Brown J. P. and Galasko D. (1997) The tau protein in human cerebrospinal fluid in Alzheimer's disease consists of proteolytically derived fragments. *J. Neurochem.* **68**, 430–433.

Karch C. M., Jeng A. T. and Goate A. M. (2012) Extracellular Tau levels are influenced by variability in Tau that is associated with tauopathies. *J. Biol. Chem.* **287**, 42751–42762.

Kim W., Lee S. and Hall G. F. (2010) Secretion of human tau fragments resembling CSF-tau in Alzheimer's disease is modulated by the presence of the exon 2 insert. *FEBS Lett.* **584**, 3085–3088.

Lasagna-Reeves C. A., Castillo-Carranza D. L., Guerrero-Muoz M. J., Jackson G. R. and Kayed R. (2010) Preparation and characterization of neurotoxic tau oligomers. *Biochemistry*, **49**, 10039–10041.

Lasagna-Reeves C. A., Castillo-Carranza D. L., Sengupta U., Clos A. L., Jackson G. R. and Kayed R. (2011) Tau oligomers impair memory and induce synaptic and mitochondrial dysfunction in wild-type mice. *Mol. Neurodegener.* **6**, 39.

Leugers C. J. and Lee G. (2010) Tau potentiates nerve growth factor-induced mitogen-activated protein kinase signaling and neurite initiation without a requirement for microtubule binding. *J. Biol. Chem.* **285**, 19125–19134.

Liu L., Drouet V., Wu J. W., Witter M. P., Small S. A., Clelland C. and Duff K. (2012) Trans-synaptic spread of tau pathology in vivo. *PLoS ONE*, **7**, e31302.

Ma Q. L., Zuo X., Yang F. *et al.* (2013) Curcumin suppresses soluble tau dimers and corrects molecular chaperone, synaptic, and behavioral deficits in aged human tau transgenic mice. *J. Biol. Chem.* **288**, 4056–4065.

Maeda S., Sahara N., Saito Y., Murayama S., Ikai A. and Takashima A. (2006) Increased levels of granular tau oligomers: an early sign of brain aging and Alzheimer's disease. *Neurosci. Res.* **54**, 197–201.

Maeda S., Sahara N., Saito Y. *et al.* (2007) Granular tau oligomers as intermediates of tau filaments. *Biochemistry*, **46**, 3856–3861.

Magnoni S., Esparza T. J., Conte V., Carbonara M., Carrabba G., Holtzman D. M., Zipfel G. J., Stocchetti N. and Brody D. L. (2012) Tau elevations in the brain extracellular space correlate with reduced amyloid-beta levels and predict adverse clinical outcomes after severe traumatic brain injury. *Brain*, **135**, 1268–1280.

Meraz-Rios M. A., Lira-De Leon K. I., Campos-Pena V., De Anda-Hernandez M. A. and Mena-Lopez R. (2010) Tau oligomers and aggregation in Alzheimer's disease. *J. Neurochem.* **112**, 1353–1367.

Morris M., Maeda S., Vossel K. and Mucke L. (2011) The many faces of tau. *Neuron*, **70**, 410–426.

Nixon R. A., Cataldo A. M. and Mathews P. M. (2000) The endosomal-lysosomal system of neurons in Alzheimer's disease pathogenesis: a review. *Neurochem. Res.* **25**, 1161–1172.

Nixon R. A., Wegiel J., Kumar A., Yu W. H., Peterhoff C., Cataldo A. and Cuervo A. M. (2005) Extensive involvement of autophagy in Alzheimer disease: an immuno-electron microscopy study. *J. Neuropathol. Exp. Neurol.* **64**, 113–122.

Park S. Y. and Ferreira A. (2005) The generation of a 17 kDa neurotoxic fragment: an alternative mechanism by which tau mediates beta-amyloid-induced neurodegeneration. *J. Neurosci.* **25**, 5365–5375.

Patterson K. R., Remmers C., Fu Y. *et al.* (2011) Characterization of prefibrillar Tau oligomers in vitro and in Alzheimer disease. *J. Biol. Chem.* **286**, 23063–23076.

Plouffe V., Mohamed N. V., Rivest-McGraw J., Bertrand J., Lauzon M. and Leclerc N. (2012) Hyperphosphorylation and cleavage at D421 enhance tau secretion. *PLoS ONE*, **7**, e36873.

Ramser E. M., Gan K. J., Decker H., Fan E. Y., Suzuki M. M., Ferreira S. T. and Silverman M. A. (2013) Amyloid-β oligomers induce tau-independent disruption of BDNF axonal transport via calcineurin activation in cultured hippocampal neurons. *Mol. Biol. Cell*, **24**, 2494–2505.

Rapoport M., Dawson H. N., Binder L. I., Vitek M. P. and Ferreira A. (2002) Tau is essential to beta -amyloid-induced neurotoxicity. *Proc. Natl Acad. Sci. USA*, **99**, 6364–6369.

Ringman J. M., Younkin S. G., Pratico D. *et al.* (2008) Biochemical markers in persons with preclinical familial Alzheimer disease. *Neurology*, **71**, 85–92.

Rissman R. A., Poon W. W., Blurton-Jones M., Oddo S., Torp R., Vitek M. P., LaFerla F. M., Rohn T. T. and Cotman C. W. (2004) Caspase-cleavage of tau is an early event in Alzheimer disease tangle pathology. *J. Clin. Invest.* **114**, 121–130.

Roberson E. D., Scearce-Levie K., Palop J. J., Yan F., Cheng I. H., Wu T., Gerstein H., Yu G. Q. and Mucke L. (2007) Reducing endogenous tau ameliorates amyloid beta-induced deficits in an Alzheimer's disease mouse model. *Science*, **316**, 750–754.

Roberson E. D., Halabisky B., Yoo J. W. *et al.* (2011) Amyloid-beta/Fyn-induced synaptic, network, and cognitive impairments depend on tau levels in multiple mouse models of Alzheimer's disease. *J. Neurosci.* **31**, 700–711.

van Rossum I. A., Visser P. J., Knol D. L., van der Flier W. M., Teunissen C. E., Barkhof F., Blankenstein M. A. and Scheltens P. (2012) Injury markers but not amyloid markers are associated with rapid progression from mild cognitive impairment to dementia in Alzheimer's disease. *J. Alzheimers Dis.* **29**, 319–327.

Sahara N., Maeda S., Murayama M., Suzuki T., Dohmae N., Yen S. H. and Takashima A. (2007) Assembly of two distinct dimers and higher-order oligomers from full-length tau. *Eur. J. Neurosci.* **25**, 3020–3029.

Saman S., Kim W., Raya M. *et al.* (2012) Exosome-associated tau is secreted in tauopathy models and is selectively phosphorylated in cerebrospinal fluid in early Alzheimer disease. *J. Biol. Chem.* **287**, 3842–3849.

Saman S., Lee N. C., Inoyo I., Jin J., Li Z., Doyle T., McKee A. C. and Hall G. F. (2014) Proteins recruited to exosomes by tau overexpression implicate novel cellular mechanisms linking tau secretion with Alzheimer's disease. *J. Alzheimers Dis.* **40**(Suppl 1), S47–S70.

Sanders D. W., Kaufman S. K., DeVos S. L. *et al.* (2014) Distinct tau prion strains propagate in cells and mice and define different tauopathies. *Neuron*, **82**, 1271–1288.

Santacruz K., Lewis J., Spires T. *et al.* (2005) Tau suppression in a neurodegenerative mouse model improves memory function. *Science*, **309**, 476–481.

Schmid I., Uittenbogaart C. H. and Giorgi J. V. (1991) A gentle fixation and permeabilization method for combined cell surface and intracellular staining with improved precision in DNA quantification. *Cytometry*, **12**, 279–285.

Sokolow S., Luu S. H., Headley A. J., Hanson A. Y., Kim T., Miller C. A., Vinters H. V. and Gylys K. H. (2011) High levels of synaptosomal Na(+)-Ca(2 +) exchangers (NCX1, NCX2, NCX3) co-localized with amyloid-beta in human cerebral cortex affected by Alzheimer's disease. *Cell Calcium*, **49**, 208–216.

Sokolow S., Henkins K. M., Bilousova T., Miller C. A., Vinters H. V., Poon W., Cole G. M. and Gylys K. H. (2012a) AD synapses contain abundant Abeta monomer and multiple soluble oligomers, including a 56-kDa assembly. *Neurobiol. Aging*, **33**, 1545–1555.

Sokolow S., Henkins K. M., Williams I. A., Vinters H. V., Schmid I., Cole G. M. and Gylys K. H. (2012b) Isolation of synaptic terminals from Alzheimer's disease cortex. *Cytometry A*, **81**, 248–254.

Sokolow S., Luu S. H., Nandy K., Miller C. A., Vinters H. V., Poon W. W. and Gylys K. H. (2012c) Preferential accumulation of amyloid-beta in presynaptic glutamatergic terminals (VGluT1 and VGluT2) in Alzheimer's disease cortex. *Neurobiol. Dis.* **45**, 381–387.

Tai H. C., Serrano-Pozo A., Hashimoto T., Frosch M. P., Spires-Jones T. L. and Hyman B. T. (2012) The synaptic accumulation of hyperphosphorylated tau oligomers in Alzheimer disease is associated with dysfunction of the ubiquitin-proteasome system. *Am. J. Pathol.* **181**, 1426–1435.

Tashiro K., Hasegawa M., Ihara Y. and Iwatsubo T. (1997) Somatodendritic localization of phosphorylated tau in neonatal and adult rat cerebral cortex. *NeuroReport*, **8**, 2797–2801.

Thies E. and Mandelkow E. M. (2007) Missorting of tau in neurons causes degeneration of synapses that can be rescued by the kinase MARK2/Par-1. *J. Neurosci.* **27**, 2896–2907.

Vossel K. A., Zhang K., Brodbeck J., Daub A. C., Sharma P., Finkbeiner S., Cui B. and Mucke L. (2010) Tau reduction prevents Abeta-induced defects in axonal transport. *Science*, **330**, 198.

Wang Y. P., Biernat J., Pickhardt M., Mandelkow E. and Mandelkow E. M. (2007) Stepwise proteolysis liberates tau fragments that nucleate the Alzheimer-like aggregation of full-length tau in a neuronal cell model. *Proc. Natl Acad. Sci. USA*, **104**, 10252–10257.

Wilhelm B. G., Mandad S., Truckenbrodt S. *et al.* (2014) Composition of isolated synaptic boutons reveals the amounts of vesicle trafficking proteins. *Science*, **344**, 1023–1028.

Wolf M. E. and Kapatos G. (1989) Flow cytometric analysis of rat striatal nerve terminals. *J. Neurosci.* **9**, 94–105.

Yamada K., Holth J. K., Liao F. *et al.* (2014) Neuronal activity regulates extracellular tau in vivo. *J. Exp. Med.* **211**, 387–393.

Yin H. and Kuret J. (2006) C-terminal truncation modulates both nucleation and extension phases of tau fibrillization. *FEBS Lett.* **580**, 211–215.

Yuan A., Kumar A., Peterhoff C., Duff K. and Nixon R. A. (2008) Axonal transport rates in vivo are unaffected by tau deletion or overexpression in mice. *J. Neurosci.* **28**, 1682–1687.

Zhang Z., Song M., Liu X. *et al.* (2014) Cleavage of tau by asparagine endopeptidase mediates the neurofibrillary pathology in Alzheimer's disease. *Nat. Med.* **20**, 1254–1262.